Shape modification of bridge cables for aerodynamic vibration control

Kleissl, Kenneth; Georgakis, Christos T.

Published in:
Proceedings of SEMC, Cape Town, Sep. 2010

Publication date:
2010

Citation (APA):
Kleissl, K., & Georgakis, C. (2010). Shape modification of bridge cables for aerodynamic vibration control. In Proceedings of SEMC, Cape Town, Sep. 2010

Shape modification of bridge cables for aerodynamic vibration control

K. Kleissl & C.T. Georgakis
Department of Civil Engineering, Technical University of Denmark, Kgs. Lyngby, Denmark

In this paper, the viability of modifying cable shape and surface for the purpose of controlling wind-induced vibrations is examined. To this end, an extensive wind-tunnel test campaign was carried out on various cable sections in the critical Reynolds number region under both smooth and turbulent flow conditions. Shape modifications of a plain cylinder included waviness, faceting and shrouding. The aerodynamic damping of each section is evaluated by applying 1- and 2-DOF quasi-steady aerodynamic models, which allow for the prediction of regions of aerodynamic instability. Whilst the plain, wavy and faceted cylinders are found to suffer from either dry inclined galloping, ”drag crisis” or Den Hartog galloping, the shrouded cylinder is found to be completely stable for all wind angles of attack, albeit with a slight increase in drag at traditional design wind velocities. The wavy cylinder is found to eliminate the risk of dry inclined galloping, with a reduction in lift fluctuations. Nevertheless, the particular cylinder is at risk of “drag crisis” instability. Finally, turbulent flow is shown to introduce a significant amount of aerodynamic damping by proving a more stable lift force over tested wind velocities.

1 INTRODUCTION

Through improved bridge monitoring and a greater openness between bridge owners and engineers, it has become increasingly apparent that a large number of the world’s long-span cable-supported bridges suffer some form of cable vibration (Kumarasena et al. 2007). These vibrations have the potential to lead to long-term fatigue damage and economic loss, through a reduction of consumer confidence. Examples of bridges with a history of cable vibrations include the First and Second Severn Crossings, Øresund Bridge, Great Belt East Bridge, Humber Bridge and the Fred Hartman Bridge.

Attempts to eliminate or dampen these vibrations have been met with varying degree of success. To date no ultimately successful cable vibration control system has been devised for all types of cable under all conditions. This is most probably due to the fact that the observed vibrations are a result of varying excitation mechanisms, several of which may need differing control strategies to combat. Tested control systems have included cable-ties, viscous/magnetoreological dampers, tuned mass dampers, spiral strands and dimples.

Nevertheless, recent work on aerodynamic control of cables through cross-sectional shape modification has shown great promise. Aerodynamic control refers to the means of eliminating undesirable vibrations of a structure through careful modification of the structural shape and surface, either passively or actively. Kleissl (2009) recently showed that circular cylinders that exhibit galloping instability, at specific wind angles of attack, can be modified passively so that these instabilities are eliminated altogether.

This paper is part of the preliminary investigations of an ongoing research project, with the objective of examining the viability of modifying cable shape and surface, for the elimination of not only cable galloping, but also vibrations due to vortex shedding - always under the prevalent meteorological conditions in Scandinavia.

2 EXPERIMENTAL INVESTIGATION

The experiments undertaken for varying flow conditions, angles of attack and cable inclination were performed at the closed circuit wind tunnel facility at FORCE Technology, Lyngby, Denmark. The test section has a height of $0.70\,\mathrm{m}$ and a width of $1.00\,\mathrm{m}$. The wind tunnel can produce a maximum wind velocity of $60\,\mathrm{m/\,s}$ in smooth flow ($< 1\%$ turbulence intensity) and $35\,\mathrm{m/\,s}$ in turbulent flow with an intensity of approximately 7%. Turbulence is generated through a turbulence grid installed upstream of the test section.

An inclined test rig, as shown in Fig. 1, was designed so that cable models could be tested at varying cable-wind angle ϕ in the range $60^\circ - 90^\circ$, where this flow angle ϕ is defined so that $\phi = 90^\circ$ correspond to flow perpendicular to the cable axis, as shown in Fig. 2. To minimize the error on the force coefficients due to end effects, the results are corrected based on measurements made with only the arms of the inclined setup installed. Finally, to ensure the end-effects did not affect the results, tests undertaken on a perpendicular section were compared with and without the use of the inclined test rig. The comparison was favouable, although a slight increase in drag was observed when using the inclined test rig. Based on a literature review of the different types of cable surface modifications (Kleissl 2009), three types of modified sections were chosen for further wind tunnel investigation. Furthermore, a plain circular cylinder was included in the test program as a reference case. The modified sections chosen for testing are shrouded, wavy and faceted hexagonal cylinders (Fig. 3).

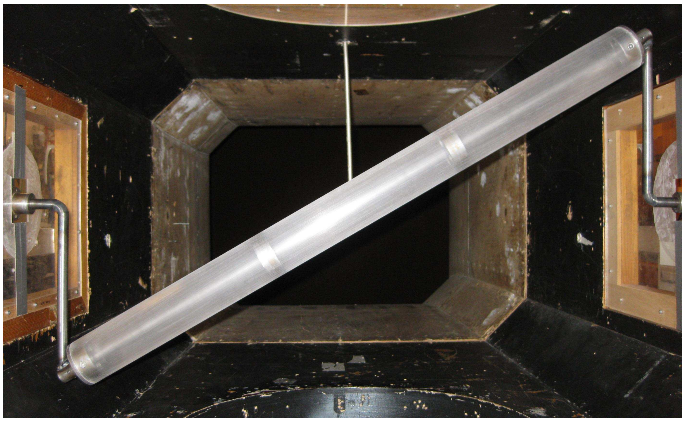

Figure 1: Illustration of the test rig.

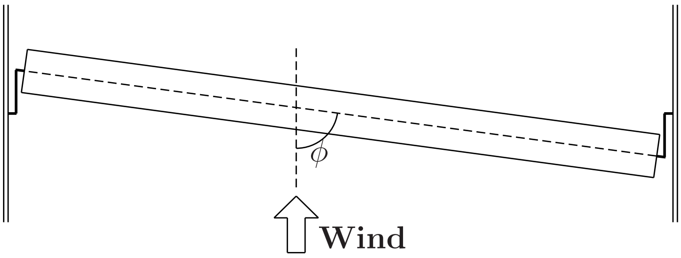

Figure 2: Plan view of the cable-wind angle ϕ.

Figure 3: Section models (from right to left), plain cylinder, wavy cylinder, faceted cylinder and shrouded cylinder.

3 TEST RESULTS

Only the force coefficients from the smooth flow tests with $\phi = 90°$ are presented herewith. As a basis for the performance evaluation of the modified sections, all force coefficients are determined using the internal circular diameter, which is the same for all sections. The results presented are corrected for a test section blockage of 10%.

The drag, lift and moment coefficients obtained for a slightly roughened cylinder in smooth flow are presented at Fig. 4. A slight roughening of the surface of the cylinder was introduced to emmulate surface pollutants that might be found on an actual bridge cable. The roughness had the added effect of ensuring that the cylinder´s critical Reynolds number region fell within the testable wind velocity range. Furthermore, the increased surface roughness produced an increased minimum drag coefficient of around 0.6 (instead of 0.3 for a perfectly smooth cylinder), as often specified for bridge design. From Fig. 4, it can be seen that the lift coefficient strongly indicates the existence of a single separation bubble precisely within the critical Reynolds number range for drag.

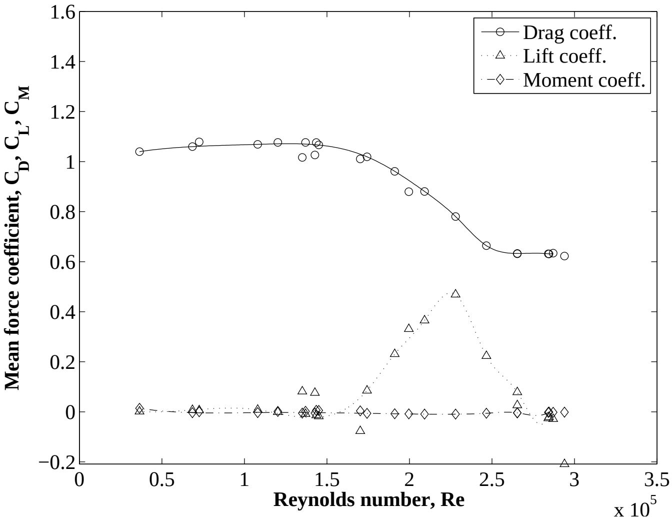

Figure 4: Force coefficients for the plain cylinder for flow $\phi = 90°$.

The results for the wavy cylinder in the smooth flow, shown in Fig. 5, look overall very much like a typical circular cylinder with a significant amount of surface roughness. The transition to the turbulent shear layer happens earlier and the dip in drag is even steeper than for the plain cylinder, although this could be the result of the surface of the RPT (Rapid Prototyping) material being slightly rougher. The drag coefficient lies around 1.2 in the subcritical region, but only drops to approx. 0.7 at the end of the critical region and slowly climbs up again through the supercritical region. A small single separation bubble can be observed from the lift coefficient, but with less than half the magnitude of the one observed for the plain circular cylinder, indicating that the waviness does reduce the vortex correlation along the cylinder axis.

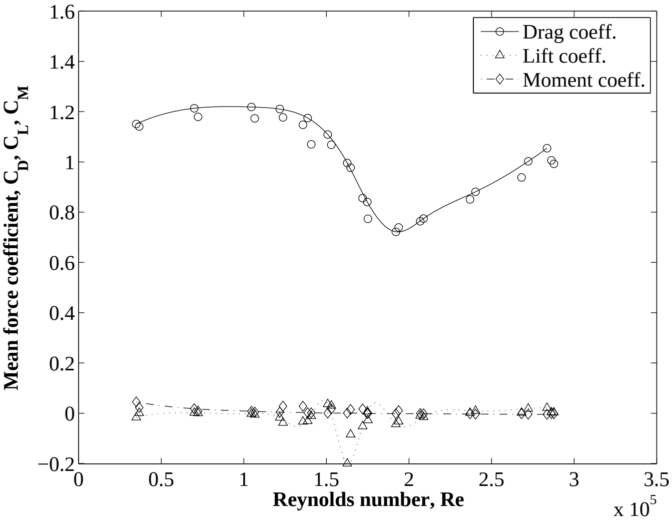

Figure 5: Force coefficients for wavy cylinder for flow $\phi = 90°$.

The faceted cylinder is not presented as the drag is found to be independent of Reynolds numbers and in the range of $1.5 - 2.0$, which is too high to be used on an actual bridge. The cylinder did also experience significant variation in drag over angle of attack, which led to the prediction of Den Hartog galloping.

In smooth flow the results for the shrouded cylinder (see Fig. 6) shows that the shroud eliminates the Reynolds number dependency. The almost constant drag coefficient slightly above 1.0 based on the inner cylinder diameter is not as low as expected. Tests described in the literature review (Kleissl 2009) indicates that a constant drag coefficient lower than 0.9 should be possible with the an efficient shroud design. With the lack in the understanding of the different shroud parameters and the "optimal" design covering a relative wide parameter region, an additional reduction of the drag coefficient should be possible by further development of the shroud by mainly focusing on drag reduction instead of reducing vortex-formations. The lift coefficient are found completely steady compared to the two other cylinders, indicating that the shrouding successfully disrupts the coherence of the vortex formation.

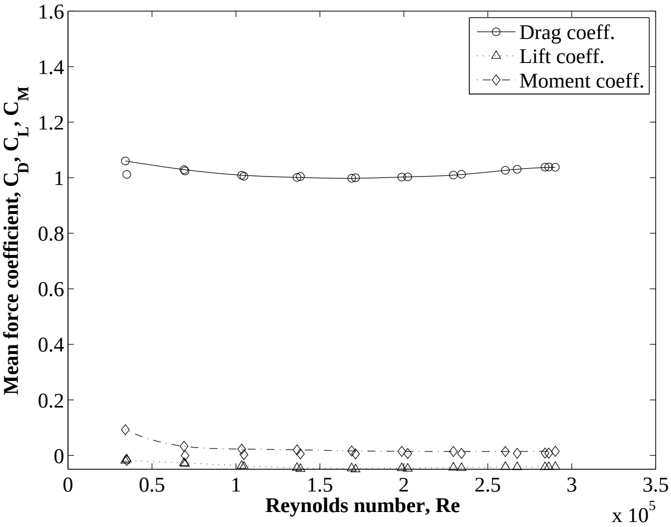

Figure 6: Force coefficients for shrouded cylinder for flow $\phi = 90°$.

4 INSTABILITY ANALYSIS

The aerodynamic damping of the tested cylinders have been evaluated by applying both 1- and 2-DOF quasi-steady aerodynamic instability models (Macdonald and Larose 2006; Macdonald and Larose 2008a). Though in this paper only the plots from the 1-DOF instability model are presented as the 2-DOF model leads to similar observations. The reasons for applying both models is that when a system starts getting detuned, it asymptotically moves towards the 1-DOF solution covering perfectly tuned systems (Macdonald and Larose 2008b). So by considering both models, both stay cables and hangers are covered.

The evaluation of instability is based purely on the aerodynamic damping in the nondimensional form, ignoring any form of structural damping. The nondimensional aerodynamic damping parameter Z_a is defined as

$$Z_a = \frac{\zeta_a m f_n}{\mu} \tag{1}$$

where ζ_a is the aerodynamic damping, m is mass per unit length, μ is the dynamic fluid viscosity and $f_n = \omega_n / 2\pi$ where ω_n is the undamped natural frequency. By using this nondimensional aerodynamic damping parameter a function is obtained that is only dependent on the Reynolds number, the cable-wind angle ϕ and the angle of attack α. In both of the stability plots, the evaluation of the aerodynamic damping is computed based on splined field approximations of the force coefficients from the inclined tests. The continuous contour line represents the transition to negative aerodynamic damping and thus the risk of instability in the case of neglectable structural damping.

From the stability plot of the plain circular cylinder, shown in Fig. 7, instability regions clearly emerges in the critical Reynolds number region and are mainly the result of the sudden dip in the drag coefficient i.e. "drag crisis" instability. Both models also predict some instability at the edge of the tested yawing range which appear outside the critical region. The fact that the models predict large instability regions for the plain cylinder at skew winds is to be expected, as several preceding investigations already have pointed this problem out as dry inclined galloping. Matsumoto et al. observed galloping instability as a result of an artificial axial flow corresponding to yawed angles in the range of $45° - 60°$. This corresponds well with the observed instability region occurring at the edge of the tested yawed angles of $60°$.

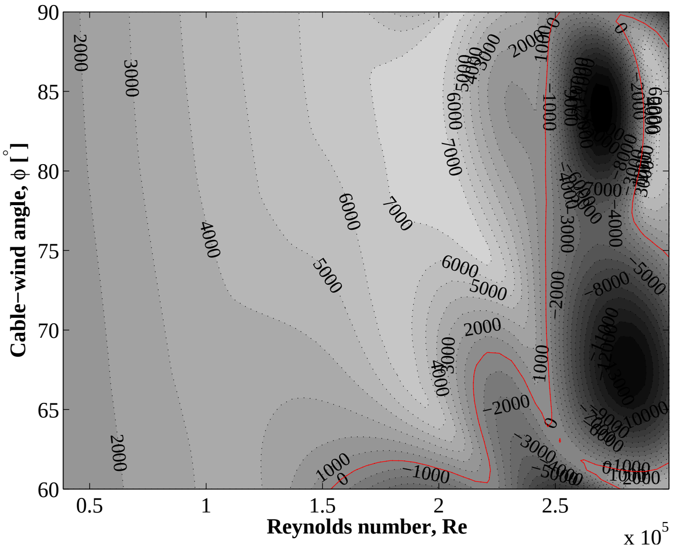

Figure 7: Nondimensional aerodynamic damping for plain circular cylinder in yawed smooth flow.

For the wavy cylinder the results for the aerodynamic damping are shown in Fig. 8. For this the instability region are seen to be very localized around the critical Reynolds number region. But because the waviness significantly reduces the secondary axial flow, the section appears more stable outside the critical Reynolds number region. This also indicates that the secondary axial flow plays an important role regarding dry inclined galloping. Never the less the wavy cylinder has some unattractive aerodynamic properties in the critical region, where "drag crisis" instability is predicted.

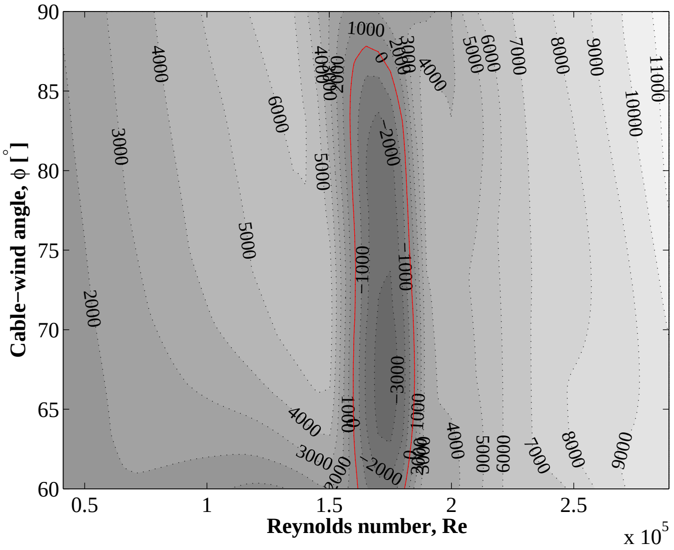

Figure 8: Nondimensional aerodynamic damping for wavy cylinder in yawed smooth flow.

The stability plot for the shrouded cylinder is not presented as the cylinder is predicted to be completely stable in the whole parameter range considered. So besides the slight increase in drag, the shroud appears very effective at aerodynamic vibration control of the cylinder.

5 CONCLUSIONS

The evaluation of aerodynamic instability shows that the plain cylinder could be prone to both "drag crisis" and dry inclined galloping at specific skew winds. The wavy cylinder have the properties similar to a typical rough circular cylinder where no significant drag increase is found, indicating some effectiveness of the waviness. The steep dip in drag results in the prediction of a "drag crisis" instability. Outside the critical Reynolds number region, it is more stable than the plain cylinder which could be a result of the reduced axial flow. The hexagonal faceted cylinder had too large a drag coefficient $(1.5 - 2.0)$ and depending on the angle of attack and the angular variation of the geometry, Den Hartog galloping is predicted. The shrouded cylinder is found to have a very low dependency on the Reynolds number and a drag coefficient slightly above 1.0 based on the inner diameter. The shroud is found to stabilize the cylinder against any type of dry state instability and it also significantly reduces the vortex-induced oscillating lateral forces. Finally, turbulent flow is shown to introduce a significant amount of aerodynamic damping by proving a more stable lift force over tested Reynolds numbers.

REFERENCES

Kleissl, K. (2009, Aug). Vibration control of bridge cables. Master's thesis, DTU Byg, DTU, Building 118, Brovej, 2800 Kgs. Lyngby, Denmark.

Kumarasena, S., N. P. Jones, P. Irwin, and P. Taylor (2007, Aug). Wind-induced vibration of stay cables. Report FHWA-HRT-05-083, US Federal Highway Administration.

Macdonald, J. H. G. and G. L. Larose (2006). A unified approach to aerodynamic damping and drag/lift instabilities, and its application to dry inclined cable galloping. *Journal of Fluids and Structures 22*(2), 229 – 252.

Macdonald, J. H. G. and G. L. Larose (2008a). Two-degree-of-freedom inclined cable galloping–part 1: General formulation and solution for perfectly tuned system. *Journal of Wind Engineering and Industrial Aerodynamics 96*(3), 291 – 307.

Macdonald, J. H. G. and G. L. Larose (2008b). Two-degree-of-freedom inclined cable galloping–part 2: Analysis and prevention for arbitrary frequency ratio. *Journal of Wind Engineering and Industrial Aerodynamics 96*(3), 308 – 326.